Journal of Operation and Automation in Power Engineering
Vol. 6, No. 2, Dec. 2018, Pages: 208-217
http://joape.uma.ac.ir

A New Method for Computation of Axial Flux Permanent Magnet Synchronous Machine Inductances under Saturated Condition.

D. Habibinia, M. R. Feyzi, and N. Rostami*

Faculty of Electrical and Computer Engineering, University of Tabriz, Tabriz, Iran.

Abstract- *Accurate computing of the saturated inductances of Permanent Magnet Synchronous Machine (PMSM) is very important during the design process. In this paper, a new method is presented based on the B-H characteristic of the stator material and unsaturated inductances formulations. This method is used to calculate the saturated inductances of the axial flux PMSM. The synchronous inductance and all of the leakage inductances can be calculated using this method. Two motors with different slot/pole combinations are selected as the case studies. The effectiveness and accuracy of the method is confirmed by 3D Finite Element Analysis (FEA). This method can be extended to other types of electric machines comprising multi-phase winding in their armature such as induction motors and other types of synchronous motors.*

Keyword: Finite element analysis, Permanent magnet synchronous Machine, Saturated inductances, Saturation.

NOMENCLATURE

A_{sc}	Slot cross section.
B_m	Peak value of air gap magnetic flux density.
L_{sd}	Direct axis synchronous inductance.
L_{sq}	Quadrature axis synchronous inductance.
L_m	Magnetizing inductance.
L_l	Leakage inductance.
L_{l-slot}	Slot leakage inductance.
L_{l-tt}	Tooth tip leakage inductance.
L_{l-EW}	End winding Leakage inductance.
$L_{l-\delta}$	Harmonic leakage inductance.
L_m^{sat}	Magnetizing inductance.
L_{l-slot}^{sat}	Slot leakage inductance.
L_{l-tt}^{sat}	Tooth tip leakage inductance.
L_{l-EW}^{sat}	End winding Leakage inductance.
$L_{l-\delta}^{sat}$	Harmonic leakage inductance.
N_{ph}	Number of turns series in phase of one stator.
S	Number of stator slots.
g_d	Effective air gap length.
k_{sat}	Saturation coefficient.
k_w	Winding factor.
l_{stator}	Stator radial length (in axial flux motor).
m	Number of phase.
p	Number of poles.
q	Slot per pole per phase.
α_i	Average to maximum value of gap flux density.
$\beta_{magnetization}$	Beta function for Magnetization inductance.
β_{l-slot}	Beta function for slot leakage.
β_{l-tt}	Beta function for tooth tip leakage.
β_{l-EW}	Beta function for end winding leakage.
λ_{slot}	Slot permeance factor.
ε	Winding short peaching ratio.
Θ_s	Stator current linkage.
τ_{ci}	Coil pitch in inner radii.
τ_{co}	Coil pitch in outer radii.
τ_p	Average pole pitch.
σ	Harmonic leakage factor.

Received: 07 Dec. 17
Revised: 04 Apr. 18
Accepted: 08 May. 18
∗Corresponding author: Davod Habibinia
E-mail: Habibinia@tabrizu.ac.ir (D. Habibinia)
Digital object identifier: 10.22098/joape.2006.4171.1324

1. INTRODUCTION

The computation of inductances in electric machines, can be studied from two different aspects. The first one is controlling viewpoint, in which, the calculated inductances (mainly the d and q axis synchronous inductances) are used to control the machine by the converter, or are used to simulate the transient or steady

state behavior of the machine during different load conditions or fault occurrence. The second aspect is due to designing viewpoint, in which the designer calculates the inductances (mainly all the leakage inductances and the synchronous inductance) of the machine by means of equations in order to use them in the design optimization or preprocessing of the machine's behavior. The methods used in the controlling viewpoint are mainly based on the measurement of the flux or the finite element analysis. They primarily calculate the synchronous inductance and do not emphasize on the leakage inductances calculations, because it is the synchronous inductance that could affect the maximum torque production capability of the machine and it is sufficient from the controller viewpoint. Also these methods rarely consider the saturation effect on the inductance value. All of these aspects can be seen in the works done previously [1-6]. Whereas, from the designer viewpoint, knowing the leakage inductance values especially the harmonic leakage inductance in the tooth-wound PMSMs, are very important. So the designer should have a simple relation-based method to be able to compute frequently the inductances during the optimization or designing program. Therefore, the computation of leakage inductances is one of the most important stages of electrical machines design and are rarely studied by the literatures [7-9]. Therefore this paper mainly concentrated on the design process requirements and focused on axial flux topology.

Some of the mentioned relations for computing inductances in the literatures are mainly based on empirical equations [10-14], such as the relations for computing end winding leakage inductance. The other equations use some assumptions such as linearized B-H characteristic, ignoring the flux fringing in the edges of the air gap and assuming sinusoidal distribution of magnetic flux density in the air gap [7-12, 15]. Consequently, the computed values are not precise enough compared to FEA results or experimental measurements [7, 15, 16].

In [7] the synchronous and leakage inductances of tooth-wound PMSM are extracted, and are also compared by the measured values. However, the selected machine is a radial flux machine, and the saturation effect is not considered to compute the inductances under heavy load conditions. The author implies that the calculation of the saturated inductances can be done by FEA.

In [1], a FEA based method is introduced to compute the synchronous inductance and the cross- saturation caused by the d and q axis currents. Anyway, this is a FEA based method and not the computational method so it could not be used by the designers in the designing program of the machine. Also the paper considers the only synchronous inductance and not the leakage ones. Furthermore, the method could be used to calculate the cross-saturation, and not applicable to compute saturation of self-inductances. Meanwhile, the method is a controlling based one. In [17, 18] the effect of slot/pole combination are studied to compute both leakage and d-q axis inductances of PMSM. It has also illustrated that, there are some appropriate slot/pole combinations considering the value of the leakage inductance and the saliency ratio of the machine.

In almost all of the aforementioned researches on the subject, the inductances are computed based on the unsaturated stator and linear B-H characteristic of the machine. Consequently, unsaturated inductances are the only computable inductances in designing procedure. Also the synchronous inductance is the only computed inductance in many of these researches. Therefore, regarding these researches the only way to evaluate the saturated inductances seems to be FEA. In other words, after extracting the motor dimensions during the design procedure, designer would be able to analyze the machine using FEA to extract exact inductances and to evaluate saturation effect on them. Therefore, finding a method to approximate the inductance behavior in saturated condition would be very useful for designers. Unfortunately, there are a few studies in this area and most of the papers evaluate the saturated inductances by only the FEA [19-21]. The few works that compute saturated synchronous inductances are based on the defining a flux path for a specific machine configuration [22]. Because of the complicated behavior of the flux in saturated conditions, these methods would be too difficult to implement in designing stage. Furthermore, it may be applicable only for specific configurations or to compute a specific inductance, like the slot leakage inductance as mentioned in [15].

Taking into account all mentioned features, the new aspects of this work are as below:

- Considering axial flux topology, which is the interested and somehow new machine topology.
- Computing all leakage inductances furthermore synchronous inductance. There is harmonic leakage, tooth tip leakage, slot leakage and end-winding leakage inductances, both in unsaturated and saturated conditions.
- Introducing new verified equations to compute saturated inductances.

- Verifying the results of introduced equations by means of 3D FEA instead of 2D FEA (in other researches, 2D FEA is mainly used by designers because of its simplicity, although as we know the 3D FEA is more accurate than 2D and computing end winding leakage inductance could not be performed by 2D analysis).

In this paper a new method, based on conventional inductance equations is introduced to estimate saturated inductance values using B-H characteristic of the stator material. Furthermore, all of the leakage inductances are calculated in addition to synchronous inductance and their behavior under saturated condition are studied too. In section 2, the conventional relations to compute unsaturated inductances are summarized. In section 3, a new method is introduced to extract saturation coefficients for each inductance. Afterwards, the saturated inductances are calculated using saturation coefficients for two different motors. In section 4, the considered motors are analyzed via 3D FEA to compute exact values of inductances in both saturated and unsaturated conditions. Then, the results of FEA are compared with the results of the proposed method to study the accuracy of the model.

2. INDUCTANCES

Many researchers [10-12] consider direct and quadrature axis inductances to study PMSM (instead of using phase inductances). This is due to the advantages of d-q frame in comparison with three phase frame.

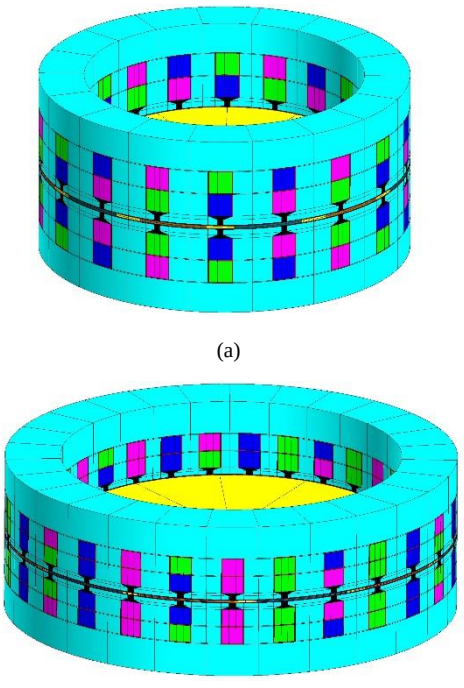

(a)

(b)

Fig. 1. Selected case studies Complete Model with two stator and sandwich rotor (a) Motor with q=0.5. (b) Motor with q=0.75.

In this paper, the considered machines are two axial flux PMSM with two stators and one rotor configuration (Fig. 1). As far as there is no saliency in the inset type rotor topology, the values of the direct and quadrature axis inductances are equal. Therefore, only the direct axis inductance is calculated. The similar way can be developed to compute quadrature axis inductance as in the interior PM topology. The synchronous direct axis inductance L_{sd} composed of two parts; the magnetizing inductance L_m and the leakage inductance L_l.

$$L_{sd} = L_m + L_l \tag{1}$$

2.1. Magnetizing Inductance

The magnetizing inductance has the main role in torque production of the machine. It can be delivered as [12]:

$$L_m = \frac{4.\alpha_i.m}{p.g_d} \times \frac{\mu_0}{\pi} \times \tau_p \times l_{stator} \times \left(k_w.N_{ph}\right)^2 \tag{2}$$

The effective air gap is calculated using Carter's coefficient as in [10].

2.2. Leakage Inductances

The leakage inductance consists of the fluxes that do not pass across the air gap and those pass across the air gap but have no role in electromagnetic power conversion. This inductance can be introduced as the sum of the other components:

$$L_l = L_{l-slot} + L_{l-tt} + L_{l-\delta} + L_{l-EW} \tag{3}$$

2.2.1. Slot leakage Inductance

The slot leakage inductance exists due to the flux lines of slot conductors that don't pass across the air gap. This inductance strongly depends on slot shape and winding type. Therefore, appropriate permeance functions have been introduced by researchers for different slot shapes [12]. For semi-open slot configuration, shown in Fig. 2, the permeance factor can be defined as:

$$\lambda_{slot} = k_1 \frac{h_4 - h'}{3b_4} + k_2\left(\frac{h_3}{b_4} + \frac{h_1}{b_1} + \frac{h_2}{b_4 - b_1} ln\left(\frac{b_4}{b_1}\right)\right) + \frac{h'}{4b_4} \tag{4}$$

Where:

$$k_1 = 1 - \frac{9}{16}\varepsilon \quad and \quad k_2 = 1 - \frac{3}{4}\varepsilon \tag{5}$$

Knowing this permeance factor, the slot leakage inductance for two stator configuration can be calculated as:

$$L_{l-slot} = \frac{8m}{S}\mu_0 l_{stator} N_{phase}^2 \times \lambda_{slot} \quad (6)$$

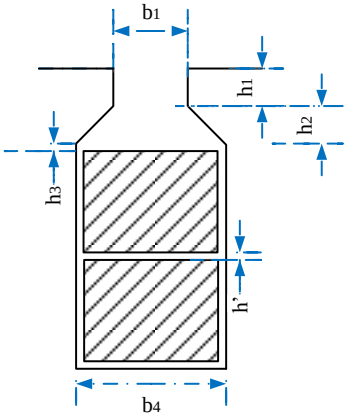

Fig. 2. The main dimensions of the machine slots.

2.2.2. Tooth tip leakage inductance

Similar to slot leakage inductance, tooth tip leakage inductance can be calculated using its own permeance function λ_{tt} and Eq. (6). This inductance depends on tooth tip shape. The corresponding tooth tip permeance function [12] is:

$$\lambda_{tt} = k_2 \frac{5\left(\frac{g}{b_1}\right)}{5+4\left(\frac{g}{b_1}\right)} \quad (7)$$

2.2.3. Harmonic leakage inductance

The harmonic leakage inductance or the air gap leakage inductance is created by mmf harmonics in the air gap region. These harmonics do not participate in electromagnetic power conversion. The value of this inductance is proportional to magnetizing inductance and the weights of mmf harmonics. The amount of this inductance is more dominant in tooth-wound machines rather than integer slot configurations [12, 23]. Therefore, to compute the harmonic leakage inductance it is sufficient to know the value of the magnetizing inductance and the weight factors of the mmf harmonics. The weight factors can also be found using harmonic winding factors. The sum of these winding factors has been introduced as a harmonic leakage factor in many literatures [7, 12].

$$\sigma = \sum_{\substack{\upsilon=1 \\ \upsilon \neq p/2}}^{\upsilon=+\infty} \left(\frac{p}{2} \cdot \frac{k_{w\upsilon}}{\upsilon . k_{wp/2}} \right)^2 \quad (8)$$

Where $k_{w\upsilon}$ denotes harmonic winding factor of order, υ and $k_{wp/2}$ is the main winding factor. Then the value of the harmonic leakage inductance can be obtained as:

$$L_{l-\delta} = \sigma \times L_m \quad (9)$$

2.2.4. End winding leakage inductance

Compared to other components of magnetic flux leakage, end winding leakage has the most complicated flux path. This is due to the variable length of flux path in both iron and air parts of the machine that totally depends on the end winding shape and also the gap between end windings tip and the stator body. Additionally, the flux path in the air parts is longer than iron parts for end winding flux leakage. Therefore end winding inductance is mostly computed based on empirical look-up tables that depends on the shape of the end windings [11, 12]. Considering arcs of the end winding [10], the following equation can be used to compute the end winding inductance:

$$L_{l-EW} = \frac{\mu_0}{2pq} N_{ph}^2 \times \left(\tau_{ci}\, ln\left(\frac{\pi.\tau_{ci}^2}{4A_{sc}}\right) + \tau_{co}\, ln\left(\frac{\pi.\tau_{co}^2}{4A_{sc}}\right) \right) \quad (10)$$

3. CONSIDERING SATURATION EFFECT

3.1. Saturation inductance calculation method

All the inductances introduced in previous section are the unsaturated values, in which the designer uses them to evaluate the machine performance or its cost functions during the design procedure. As we know, an electric motor may be affected by saturation during the short time overloads. So these equations may not be held. Therefore, designer requires some modified equations to use them in such a condition. In this section these modified equations are introduced. Most of the leakage inductances except the end winding leakage are due to the leakage fluxes that are near the iron parts, such as the slot leakage and the tooth tip leakage in which, the length of the flux path through the iron parts is longer than in the air parts. Therefore, the B-H characteristic of iron laminations of stator has the main role in inductance variations during saturation. The harmonic leakage flux because of its relation with the magnetization flux is also affected by the saturation. But the end winding flux may be less affected by the saturation because of the longer air path regarding its leakage flux as it will be illustrated by FEA. The stator material used is 0.27 mm (Neo27) low loss steel laminations. The B-H characteristic of laminations is depicted in Fig. 3. The rotor is nonmagnetic material with NdFeB magnets mounted on its surface as an inset magnets. Considering sandwich type rotor with inset magnets, non-magnetic property of the rotor body and the relative permeability of the magnets which is near to air permeability, the saliency ratio of the motor will be near

one. Therefore, only the d axis inductance are calculated with its related leakage inductances.

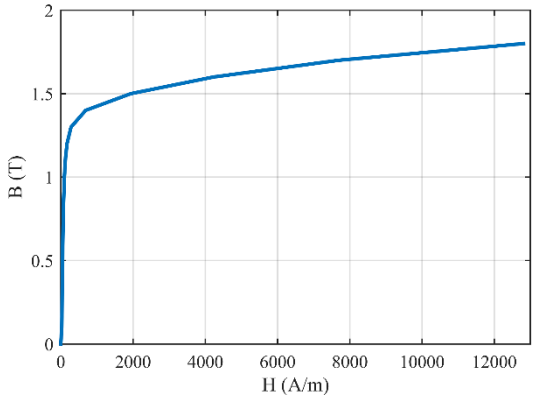

Fig. 3. B-H characteristic of Neo27 steel lamination.

Most of the rotating electric machines are designed to operate near the knee of B-H characteristic curve. Furthermore, the rate of increase in the magnetic field is proportional to current. The machine is commonly designed to operate with its rated current near the knee point considering the tooth maximum unsaturated magnetic flux density. The hard saturation usually happens when the machine reaches its maximum load. In this study the nominal current of case studies is 9 Amperes and the maximum load is 3 times of the rated current which is due to saturation level. Therefore the maximum machine load is defined considering maximum saturated flux density in the tooth of the machine. The curve in Fig. 1 consists of two linear parts. Therefore, Magnetic flux density in the air gap considering stator current linkage will be [12]:

$$B_m = \frac{\mu_0 . \Theta_s}{g_d} \tag{11}$$

The saturation coefficient is defined as the ratio of the magnetic flux density to the current linkage of the armature winding.

$$k_{sat} = \frac{B_{m-sat}}{\Theta_{s-sat}} \tag{12}$$

By studying Eqs. (2), (6) and (10), and knowing that the value of Eq. (12) can be placed instead of μ_0 / g_d, Beta functions for each inductance can be defined by eliminating the term μ_0 / g_d as below:

$$\beta_{magnetization} = \frac{4.\alpha_i . m}{\pi . p} \times \tau_p \times l_{stator} \times \left(k_w . N_{ph}\right)^2 \tag{13}$$

$$\beta_{l-slot} = \frac{8m}{S} g_d l_{stator} N_{phase}^2 \times \lambda_{slot} \tag{14}$$

$$\beta_{l-tt} = \frac{8m}{S} g_d l_{stator} N_{phase}^2 \times \lambda_{tt} \tag{15}$$

$$\beta_{l-EW} = \frac{g_d}{2pq} N_{ph}^2 \times \left(\tau_{ci} \ln\left(\frac{\pi . \tau_{ci}^2}{4A_{sc}}\right) + \tau_{co} \ln\left(\frac{\pi . \tau_{co}^2}{4A_{sc}}\right)\right) \tag{16}$$

Therefore each inductance in saturated condition can be calculated by multiplying its corresponding β function by k_{sat} as follows:

$$L_m^{sat} = \beta_{magnetization} \times k_{sat} \tag{17}$$

$$L_{l-slot}^{sat} = \beta_{l-slot} \times k_{sat} \tag{18}$$

$$L_{l-tt}^{sat} = \beta_{l-tt} \times k_{sat} \tag{19}$$

$$L_{l-EW}^{sat} = \beta_{l-EW} \times k_{sat} \tag{20}$$

$$L_{l-\delta}^{sat} = \sigma \times L_{m-sat} \tag{21}$$

To compute k_{sat}, the value of the saturation magnetic flux density that is defined for overload condition should be divided into the current linkage value of the corresponding defined overload current. The value of the current linkage can be calculated as [12]:

$$\Theta_s^{sat} = \frac{4}{\pi} . \frac{k_{ws} . N_{ph}}{p} . \sqrt{2} . I_s^{sat} \tag{22}$$

Where I_s^{sat} and Θ_s^{sat} are the overload current and the overload current linkage values, respectively.

3.2. Case studies

Two KAMAN type axial flux PMSM motors are selected to compute the saturated inductances. The considered machines structure and their windings are depicted in Fig. 4 and Fig. 5.

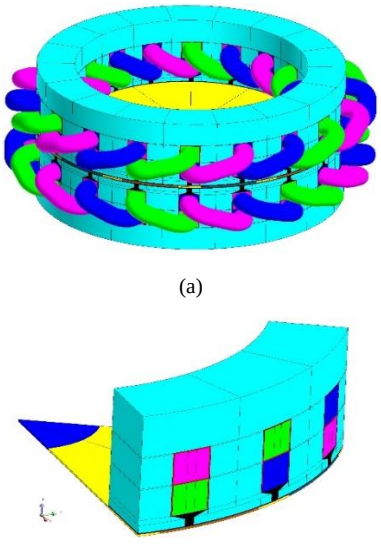

(a)

(b)

Fig. 4. First motor with q=0.5. (a) Complete model with winding (b) one sixth model with 3 slot and symmetrical Y- plane.

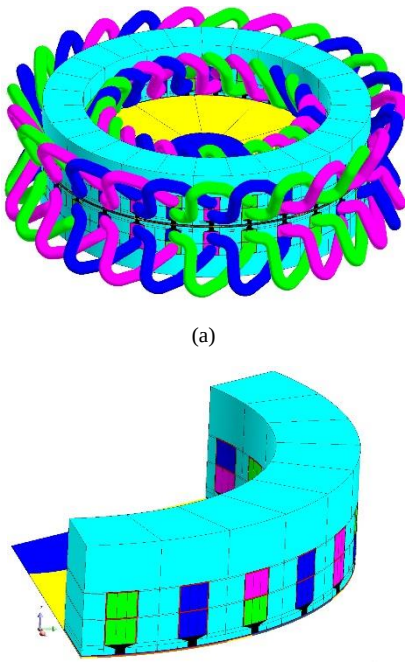

(a) (b)

Fig. 5. Second motor with q=0.75. (a) Complete model with winding (b) one third model with 9 slot and symmetrical Y- plane.

Both motors comprising two-layer winding in rectangular slots. The first motor has tooth-wound coils and its slot/pole combination equals to 18/12, the second one has the winding pitch equals to two slot, then there is a distributed winding and its slot/pole combination equals to 27/12. Other geometric parameters of these two case studies are given in Table 1.

Table 1. Considered Motors Properties

parameter	First case	Second case
p	12	12
$g\ (mm)$	0.5	0.5
$D_i\ (mm)$	164	191
$D_o\ (mm)$	217	253
S	18	27
q	0.5	0.75
N_{ph}	384	297
m	3	3
$h_1\ (mm)$	3.36	2.3
$h_2\ (mm)$	2.24	1.5
$h_3\ (mm)$	0.5	0.5
$h'\ (mm)$	0.5	0.5
$b_1\ (mm)$	3.38	3.8
$b_4\ (mm)$	14.56	12.7

Using maximum overload current of 27 Amperes and saturated level as Fig. 2, the value of k_{sat} can be calculated using Eqs. (11), (12) and (22) as 0.00032. Therefore, using equations set in previous sections (Eqs. (13) to (21)) the value of inductances in normal and saturated conditions can be calculated. These results are listed in Table 2. As we see in Table 2, increase in current value cause the saturation in both stator teeth and yoke. All of the flux paths regarding leakage inductances, close their path through both air and iron parts, therefore, similar to magnetizing inductance, these leakage inductances also experience saturation by reduction in their value. To verify the saturated inductances values in table 2, a 3D FEA are performed in next section.

Table 2. Calculated Normal and Saturated Inductances

Inductances	First case (mH)		Second case (mH)	
	No sat	sat	No sat	sat
L_m	17.21	7.52	24.56	8.63
L_{l-slot}	9.88	4.3	3.88	1.36
L_{l-tt}	2.1	0.9	0.82	0.29
L_{l-EW}	0.8	0.34	1.34	0.47
$L_{l-\sigma}$	7.93	3.46	6.66	2.34
L_l	20.71	9	12.7	4.46
L_{sd}	37.92	16.52	37.26	13.09

4. FINITE ELEMENT ANALYSIS AND RESULTS

In this section a 3D FEA are performed to validate the results obtained by analytical equations explained in previous sections. The inductances are computed based on energy method and both the static and incremental dynamic inductances are obtained by FEA.

4.1. Performing FEA

To compute each inductance component, the machine are divided to some parts and the stored energy in each part are computed by 3D FEA for current variation from zero to the overload value. The related parts for each inductance are as below:

- *Slot leakage inductance:* stored energy in the slots and insulator parts of the slots.
- *Tooth tip leakage inductance:* stored energy in the slots opening area.
- *End winding leakage inductance:* stored energy in the annular volume, containing end-winding parts inside the inner radii and outside the outer radii (slot areas are excluded).
- *Direct axis synchronous inductance:* stored total energy in the 3D domain, there is stator-rotor configuration.

By using these energies, all of the inductances can be calculated except the magnetizing inductance and the harmonic leakage inductance. To find the magnetizing inductance, based on the above inductances, the below equations can be used:

$$L_{md} + L_{l-\sigma} = L_{sd} - \left(L_{l-slot} + L_{l-tt} + L_{l-EW}\right) \tag{23}$$

$$L_{md} = \frac{L_{sd} - \left(L_{l-slot} + L_{l-tt} + L_{l-EW}\right)}{1+\sigma} \tag{24}$$

The value of the harmonic leakage inductance knowing the magnetizing inductance can be found by (9). To compute dynamic inductance by the energy method, the below relation in FEA are used for three phase winding configuration with coupling factor which equals to –0.5 for these case studies:

$$L_x = \frac{2}{3} \times \frac{1}{I} \times \frac{dW_x}{dI} \tag{25}$$

$$L_x = \frac{4}{3} \times \frac{W_x}{I^2} \tag{26}$$

In these relations, x denotes to each of the four parts that the related inductance energy are stored in. Considering symmetry and periodicity, the machines model can be reduced to a part of full model. Therefore, only one sixth of the machine structure in 18/12 configuration and one third of the machine structure in 27/12 configuration is enough to be modelled, as shown previously in Figs. 4 and 5. The rotors are also placed in the d-axis location and the stator winding is excited in such a condition to have zero value for q axis current component where $I_a = I$, $I_b = I_c = -I/2$.

Variation of the dynamic leakage inductances by the current of armature for both machines is depicted in Fig. 6 and Fig. 7.

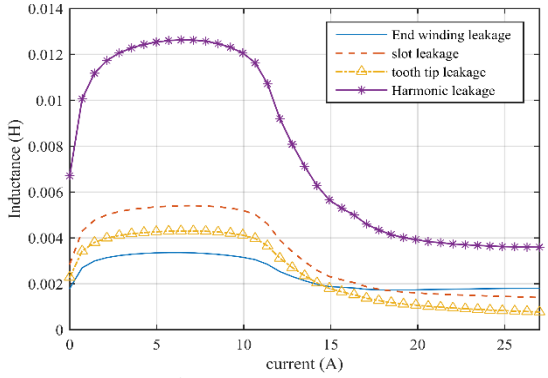

Fig. 6. Variation of dynamic leakage inductances by the armature current for the motor with q=0.5.

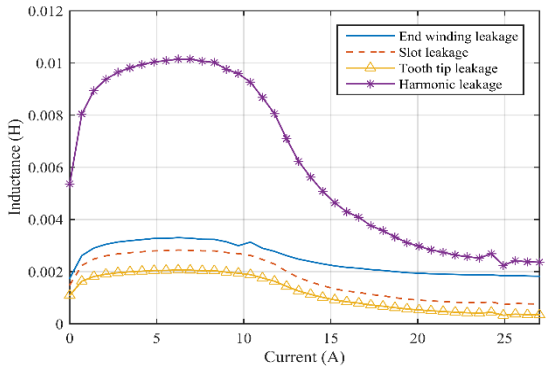

Fig. 7. Variation of dynamic leakage inductances by the armature current for the motor with q=0.75.

In both cases the harmonic leakage inductance is the dominant leakage inductance and its value is greater for 18/12 configuration compared with other one. This is due to tooth-wound winding of 18/12 machine and larger harmonic component of its air gap flux density as mentioned in [23]. The value of end-winding leakage inductance in 27/12 configuration is greater than the slot and tooth-tip leakage inductance as was shown in Fig. 7. This is due to the larger end windings of 27/12 configuration (2 slots of winding pitch), On the contrary for 18/12 machine with one slot for winding pitch, this inductance is the smallest one among the other inductances, as it is evident from Fig. 6. In both figures it can be seen that the saturation has the minimum effect on the end winding inductance. It is due to the larger space between the end windings and the iron parts of stator comparing other parts of the winding. On the other hand, a large amount of the leakage flux due to the end windings passes through the air rather than iron parts. The effect of saturation is more dominant in the slot or tooth tip leakage fluxes that pass a larger path through iron parts rather than air parts.

The static leakage inductances for both machines are also calculated using 3D FEA and Eq. (26). The results are depicted in Figs. 8 and 9.

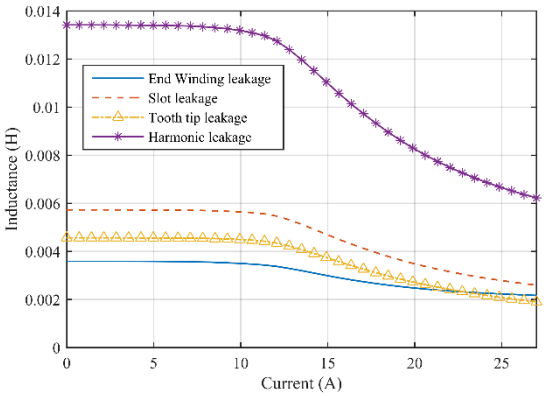

Fig. 8. Variation of static leakage inductances by the armature current for the motor with q=0.5.

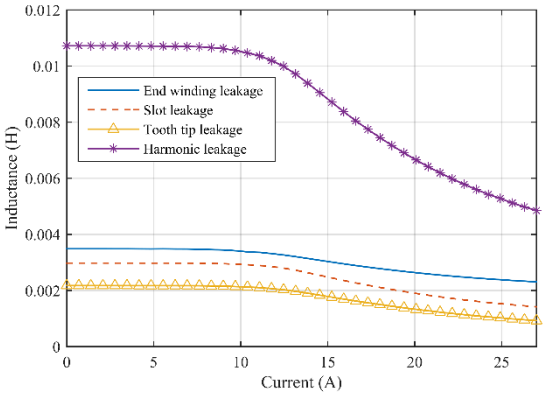

Fig. 9. Variation of static leakage inductances by the armature current for the motor with q=0.75.

The same conclusions as the dynamic results could be extracted here. For example, the value of end-winding leakage inductance comparing other inductances, has the minimum variation considering saturation. Comparing dynamic results, the saturated and unsaturated static inductances have a little larger values. This is due the nature of the static inductance computation. Also comparing static inductances, the value of the dynamic inductances have the lower values near the zero current. This is due to the lower value for the rate of the changes in the flux linkage comparing current rise in small current values. This fact, affects the rate of change in stored energy in low current values and consequently affects the inductances near the low currents by (25). In all of these figures the value of unsaturated inductances are the values corresponding to the rated current and the saturated inductances are the values regarding the maximum overload current. The rate of decrease of inductances by the current is different for each inductance. The reason is the different length of flux paths that pass across the iron parts of the machine for each inductance. It means that the longer the length of the flux path in the iron parts, the more effect of saturation on decreasing the inductances.

The direct axis inductance, the magnetizing inductance and the total leakage inductance for both motors are depicted in Fig. 10 and 11. Fig. 10 shows the variation of the static inductances and Fig. 11 shows the variation of the dynamic inductances.

Figures 10 and 11 shows that by increasing the numbers of slots per pole per phase, the total leakage inductance decreases. The main reason is the reduction of the harmonics of the air gap flux density due to distributing the windings within the more slots. However, the value of the end winding leakage flux may increase by the q, but this increase is not comparable by the decrease of harmonic leakage flux.

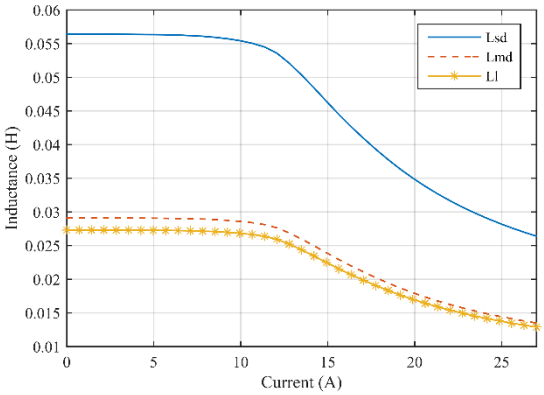

(a)

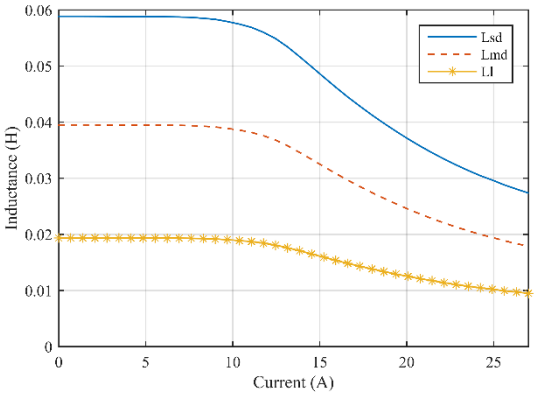

(b)

Fig. 10. Main static inductances of two case study (a) motor with q=0.5 (b) motor with q=0.75.

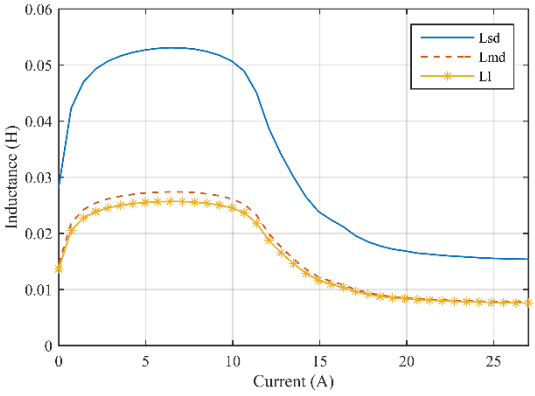

(a)

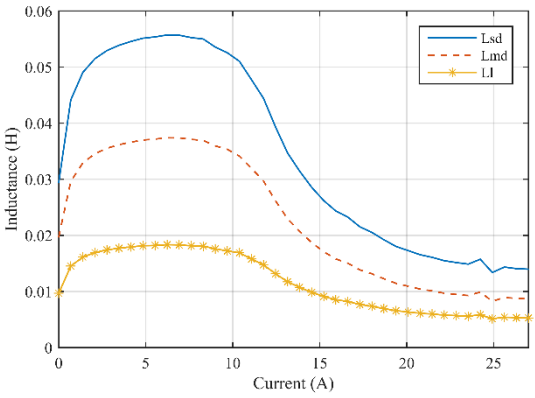

(b)

Fig. 11. Main dynamic inductances of two case study (a) motor with q=0.5 (b) motor with q=0.75.

4.2. Comparing results

The results of evaluating the normal and the saturated dynamic inductances with the equations of the section 3 and the FEA results are shown in Table 3 and 4.

It is clear from these tables that results of equations in both the normal and saturated conditions have some acceptable deflections from the more exact FEA results. This variance is due to the empirical and simplified nature of the inductance equations, which is acceptable by many designers [16, 24].

Table 3. Comparison of Normal and Saturated Dynamic Inductances with Equations and FEA for 18/12 Motor.

	Normal values (mH)		Saturated values (mH)	
	Results by	Results by	Results by	Results by
L_{l-slot}	9.88	3.4	4.3	1.4
L_{l-tt}	2.1	2.71	0.9	0.77
L_{l-EW}	0.8	2.31	0.34	1.8
$L_{l-\sigma}$	7.93	8.08	3.46	3.59
L_l	20.71	16.5	9	7.56
L_m	17.21	17.52	7.52	7.8
L_{sd}	37.92	34.02	16.52	15.36

Table 4. Comparison of Normal and Saturated Dynamic Inductances with Equations and FEA for 27/12 Motor.

	Normal values (mH)		Saturated values (mH)	
	Results by	Results by	Results by	Results by
L_{l-slot}	3.88	1.77	1.36	0.76
L_{l-tt}	0.82	1.25	0.29	0.34
L_{l-EW}	1.34	2.47	0.47	1.82
$L_{l-\sigma}$	6.66	6.23	2.34	2.35
L_l	12.7	11.72	4.46	5.27
L_m	24.56	22.95	8.63	8.69
L_{sd}	37.26	34.67	13.09	13.96

However, comparing equation results with FEA one, the similar variances like those of the unsaturated inductances exist in the saturated inductances too. Even the difference of saturated values is less than the normal values in some cases like harmonic leakage, tooth tip leakage, magnetizing inductance and synchronous inductance. Therefore the FEA results showed that the introduced equations for computing saturated inductances have enough accuracy to be used by designers in the design stage of the machine.

As it is clear from table 3 and 4, the saturated and normal values of the end winding and slot leakage inductances that are achieved by equations have the most discrepancy by FEA results comparing the other inductances. In both of them, this matter can be explained by the empirical nature of the corresponding equations. Also for the end winding inductance, the other reason is using same saturation coefficient while considering shorter flux path in the iron parts compared to other inductances. The value of saturated total leakage inductance for 18/12 machine that achieved by equation has 19% different comparing FEA results. This difference percentage for 27/12 configuration is 15.3%. The calculated saturated synchronous inductance for 18/12 configuration has 7.5% difference with FEA results and for 27/12 configuration the difference is about 6.2%. It can be seen from these tables that the difference for calculated unsaturated synchronous inductance comparing FEA results for 18/12 and 27/12 configurations is 11.46% and 7.47% respectively. These small differences, confirm the accuracy of the introduced equations.

Therefore, from the designer view point and before entering FEA stage, it is better to use such simple equations to compute the saturated inductances alongside of the normal inductances, during the design procedure or optimization programs.

5. CONCLUSION

A simple inductance calculation method based on the B-H characteristic of the stator material and the normal inductance equations are explained in this paper. The proposed method was used to find a modified equation set, to compute the saturated inductances in the first step of designing an electric machine. In this method, β functions for each inductance are created based on the unsaturated inductance equations. The way to find the saturation factor based on the designed overload current and the B-H characteristic of the machine are also explained. The same as the equation set for unsaturated inductances, these modified equations can be used by the designer to compute saturated inductances during the design step.

The method is studied on two case studies that are two axial flux PMSM with sandwich rotor, which differs in slot pole combinations. All of their inductance values are calculated by this method. To verify the method a 3D finite element analyses are executed on both machines and the normal and saturated inductances are computed using energy method by finite element analysis. Both of the static and dynamic inductances are computed by Finite element. Also the synchronous and all the leakage inductances are computed by FEA. Finally, the obtained results by the equations are compared with the exact FEA results. The results showed that the similar differences between the unsaturated equations and FEA results exists in the saturated modified equations comparing their corresponding FEA results too. It means that the results have the good accuracy and in some cases they have better discrepancy comparing FEA with respect to unsaturated equations. Therefore, considering that the normal inductance equations generally are used by designers, then this modified saturated relations with such small tolerances can also be used.

REFERENCES

[1]K. J. Meessen, P. Thelin, J. Soulard, and E. Lomonova, "Inductance calculations of permanent-magnet synchronous machines including flux change and self-and cross-saturations," *IEEE Trans. Magn.*, vol. 44, pp. 2324-2331, 2008.

[2]H. Chen, Y. Chen, S. r. Huang, and F. Zhang, "Calculation of inductance of permanent magnet synchronous motor

considering permanent magnet flux linkage variation of load conditions," Proce. *2014 IEEE Conf. Expo. Transp. Electrif. Asia-Pacific*, 2014, pp. 1-6.

[3]Y. Gao, R. Qu, C. Yu, L. Jian, and X. Wei, "Review of off-line synchronous inductance measurement method for permanent magnet synchronous machines," Proce. *2014 IEEE Conf. Expo. Transp. Electrif. Asia-Pacific*, 2014, pp. 1-6.

[4]B. Zaghdoud and A. Saadoun, "Inductances calculation of permanent magnet synchronous machine," *Int. J. Comp. Electr. Eng.*, vol. 6, p. 267, 2014.

[5]H. Zhang, B. Kou, L. Wang, Y. Jin, and H. Zhang, "A new inductance measurement method for permanent magnet synchronous linear motor," Proce. *17th Int. Conf. Electr. Mach. Syst.*, 2014, pp. 1539-1542.

[6]Y. Gao, R. Qu, and D. Li, "Improved hybrid method to calculate inductances of permanent magnet synchronous machines with skewed stators based on winding function theory," *Chin. J. Electr. Eng.*, vol. 2, pp. 52-61, 2016.

[7]P. Ponomarev, Y. Alexandrova, I. Petrov, P. Lindh, E. Lomonova, and J. Pyrhönen, "Inductance calculation of tooth-coil permanent-magnet synchronous machines," *IEEE Trans. Ind. Electr.*, vol. 61, pp. 5966-5973, 2014.

[8]B. Prieto, M. Martínez-Iturralde, L. Fontán, and I. Elosegui, "Analytical calculation of the slot leakage inductance in fractional-slot concentrated-winding machines," *IEEE Trans. Ind. Electr.*, vol. 62, pp. 2742-2752, 2015.

[9]M. Bortolozzi, A. Tessarolo, and C. Bruzzese, "Analytical computation of end-coil leakage inductance of round-rotor synchronous machines field winding," *IEEE Trans. Magn.*, vol. 52, pp. 1-10, 2016.

[10]D. C. Hanselman, *Brushless permanent magnet motor design*, 2nd ed. Cranston, R.I.: The Writers' Collective, 2003.

[11]J. F. Gieras, R.-J. Wang, M. J. Kamper, and SpringerLink (Online service). (2008). Axial flux permanent magnet brushless machines (2nd ed.). Available: http://lib-ezproxy.tamu.edu:2048/login?url=http://dx.doi.org/10.1007/978-1-4020-8227-6

[12]J. Pyrhonen, T. Jokinen, and V. Hrabovcovâa, Design of rotating electrical machines. Chichester, U.K.: Wiley, 2008.

[13]V. Behjat and A. Dehghanzadeh, "Experimental and 3D finite element analysis of a slotless air-cored axial flux PMSG for wind turbine application," *J. Oper. Autom. Power Eng.*, vol. 2, pp. 121-128, 2014.

[14]H. Nazari and N. Rostami, "Diagnosis of different types of air-gap eccentricity fault in switched reluctance motors using transient finite element method," *J. Oper. Autom. Power Eng.*, vol. 3, pp. 94-101, 2015.

[15]A. Tessarolo, "Analytical determination of slot leakage field and inductances of electric machines with double-layer windings and semiclosed slots," *IEEE Trans. Energy Convers.*, vol. 30, pp. 1528-1536, 2015.

[16]O. Chiver, E. Micu, and C. Barz, "Stator winding leakage inductances determination using finite elements method," Proce. *11th Int. Conf. Opt. Electr. Electron. Equip.*, 2008, pp. 69-74.

[17]P. Ponomarev, P. Lindh, and J. Pyrhönen, "Effect of slot-and-pole combination on the leakage inductance and the performance of tooth-coil permanent-magnet synchronous machines," *IEEE Trans. Ind. Electron.*, vol. 60, pp. 4310-4317, 2013.

[18]R. Ni, G. Wang, X. Gui, and D. Xu, "Investigation of d- and q-axis inductances influenced by slot-pole combinations based on axial flux permanent-magnet machines," *IEEE Trans. Ind. Electron.*, vol. 61, pp. 4539-4551, 2014.

[19]J. Graus, A. Boehm, and I. Hahn, "Influence of stator saturation on the differential inductances of PM-synchronous machines with concentrated winding," Proce. *3rd IEEE Int. Symp. Sensorless Control Electr. Drives*, 2012, pp. 1-7.

[20]J. Graus, S. Luthardt, and I. Hahn, "Influence of rotor saturation on the differential inductances of PM-synchronous machines with concentrated winding," Proce. *2013 15th Europ. Conf. Power Electron. Appl. (EPE)*, 2013, pp. 1-10.

[21]A. Pouramin, R. Dutta, M. F. Rahman, and D. Xiao, "Inductances of a fractional-slot concentrated-winding interior PM synchronous machine considering effects of saturation and cross magnetization," Proce. *IEEE Energy Convers. Congr. Expo.*, 2015, pp. 6075-6081.

[22]K. Shima, K. Ide, and M. Takahashi, "Finite-element calculation of leakage inductances of a saturated salient-pole synchronous machine with damper circuits," *IEEE Trans. Energy Convers.*, vol. 17, pp. 463-470, 2002.

[23]P. Ponomarev, I. Petrov, and J. Pyrhönen, "Influence of travelling current linkage harmonics on inductance variation, torque ripple and sensorless capability of tooth-coil permanent-magnet synchronous machines," *IEEE Trans.Magn.*, vol. 50, pp. 1-8, 2014.

[24]K. Shima, K. Ide, M. Takahashi, Y. Yoshinari, and M. Nitobe, "Calculation of leakage inductances of a salient-pole synchronous machine using finite elements," *IEEE Trans. Energy Convers.*, vol. 14, pp. 1156-1161, 1999.